Materials Research Bulletin 59 (2014) 154–161

Contents lists available at ScienceDirect

Materials Research Bulletin

journal homepage: www.elsevier.com/locate/matresbu

Sol–gel synthesis of silver nanocrystals embedded in sodium borosilicate monolithic transparent glass with giant third-order optical nonlinearities

Lang Pei [a], Weidong Xiang [a,*], Xiuli Zhao [a], Xiaojuan Liang [a], Xinyu Yang [a], Haitao Liu [a], Zhaoping Chen [a], Cuiping Xie [d], Xin Ma [a], Chenglong Zhang [a], Li Ma [a], Jialong Zhao [b,c]

[a] College of Chemistry and Materials Engineering, Wenzhou University, Wenzhou, Zhejiang 325035, China
[b] College of Mechanical and Electrical Engineering, Wenzhou University, Wenzhou,Zhejiang 325035, China
[c] State Key Laboratory of Luminescence and Applications, Changchun Institute of Optics, Fine Mechanics and Physics,Chinese Academy of Sciences, Changchun 130033, China
[d] College of Materials Science and Engineering, Tongji University, Shanghai 201804, China

ARTICLE INFO

Article history:
Received 13 February 2014
Received in revised form 30 May 2014
Accepted 30 June 2014
Available online 2 July 2014

Keywords:
Sol–gel
Silver nanocrystals
Glass
Z-scan
Mechanism

ABSTRACT

We report the preparation of uniform spherical shape silver nanocrystals doped sodium borosilicate monolithic transparent glass by sol–gel method. The characterization of the resulting Ag nanocrystals was accomplished by using X-ray powder diffraction, transmission electron microscopy, X-ray photoelectron spectroscopy, and energy dispersive X-ray spectrum. Surface plasma resonance absorption peaks of the silver nanocrystals glass at about 406 nm have been obtained from ultraviolet–visible absorption spectrometer and their intensity is changed with different heat treatment temperatures. We have investigated the nonlinear optical properties of silver quantum dots doped glass using Z-scan technique. Third-order nonlinear optical susceptibility $\chi^{(3)}$ of the glass was estimated to be 1.01×10^{-11} esu. In particular, a mechanism for the formation of Ag quantum dots glass is proposed. This work will significantly promote the obtained material applications in optical devices.

1. Introduction

Ultrafast all-optical switches have been demonstrated to play an important role in the next generation broadband optical networks [1,2]. In recent years, metal quantum dots glasses have been recognized as excellent candidate materials for fabricating all-optical photonic devices due to not only their ultrafast nonlinear response time and large third-order optical nonlinearities, but also their fast response speed and compatibility with the existing optical fiber systems [3–6]. Among the metal quantum dot dopants, Ag nanocrystals have attracted great attention in nanoscience and nanotechnology due to their fascinating chemical and physical properties, such as catalytic [7–9], optical [10], antibacterial [11,12], narrow plasmon band and high scattering efficiency [13]. What's more, the most conspicuous manifestation of confinement in optical properties are the appearance of the surface plasmon resonance (SPR) in the visible region that strongly enhances the third-order optical nonlinearity [14,15].

To date, a significant amount of research has been focused on Ag@SiO_2 core–shell structures materials because they combine the unique properties and promising applications of both the core materials and the shell materials [13,16–21]. In this case, the research on the third-order optical nonlinearity of Ag quantum dots glass has been lagging far behind. To the best of our knowledge, the third-order nonlinear susceptibility dispersion is for the first time measured for the case of Ag colloidal glasses around the SPR resonance in 1998 by Faccio et al. [22]. Later, Yang et al. [23] reported the preparation of Ag quantum dots glasses via ion-exchange method. The results indicate that the third-order susceptibility increases with the increasing of the annealing temperature, but the transmission electron microscopy (TEM) images indicated that Ag nanocrystals aggregation has a treelike structure. Recently, another interesting work [24] investigated the spectral dependence of both nonlinear refraction and absorption in lead–germanium oxide glasses containing silver nanocrystals, indicating that this material is suitable for all-optical switching at telecom wavelengths. However, in mostly

* Corresponding author. Tel.: +86 577 86596013; fax: +86 577 86689644.
E-mail address: xiangweidong001@126.com (W. Xiang).

http://dx.doi.org/10.1016/j.materresbull.2014.06.034
0025-5408/

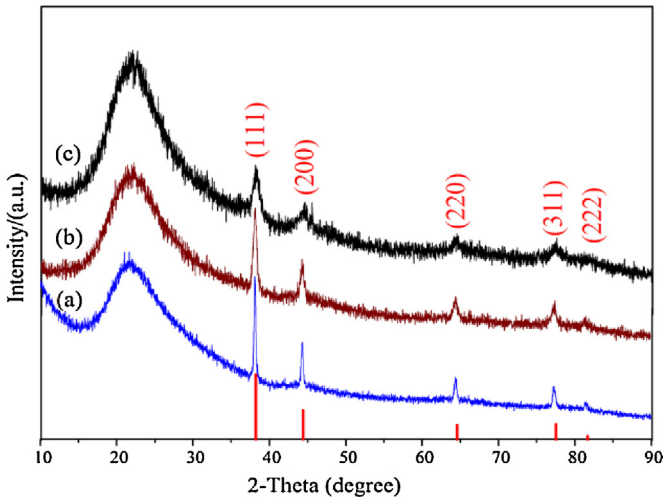

Fig. 1. XRD patterns of the Ag doped NBS glasses obtained after sintered at (a) 420 °C, (b) 450 °C and (c) 470 °C.The red lines show their standard patterns as in JCPDS card No. 65-2871.

previous studies, there always encountered a major problem that has a huge challenge to synthesize monolithic transparent metal quantum dots doped glass without fracturing, which significantly hinders their deep investigation and potential applications, particularly when used for manufacturing all-optical photonic devices. Furthermore, the high tendency to form aggregates induced by the high surface energy of the Ag nanocrystals, which causes deterioration of their chemical properties. Therefore, preparation of Ag quantum dots transparent glasses without fracturing and aggregating is essential in order to fully exploit their peculiar properties and unique applications.

To reach this aim, the use of sol–gel technique is often mentioned as a promising alternative. As we know, the sol–gel technique has the major advantages in obtaining the promising monoliths glass materials over conventional methods, such as significantly lower synthesis temperatures, the controllable composition and high chemical homogeneity of the materials, near-net-shape objects can be produced directly by casting and gelating of the sols in molds [25–27]. On the other hand, depending on how the stiff gel is sintered, the stability of the metal nanomaterials can greatly enhance and the aggregation of metal particles can be suppressed. In addition, various metal quantum dots (such as In, Cu, Bi) doped glasses [28–30] were successfully prepared by the facile sol–gel technique, and their nonlinear optical properties were carefully investigated in our previous reports.

Herein, inspired by noble metal quantum dots doped glass enhanced the optical nonlinearities, we have prepared Ag-doped sodium borosilicate (NBS) glass with Ag content ($Ag/Na_2O + B_2O_3 + SiO_2$) of 1.5 wt.% by sol–gel technique. The structure, absorption and nonlinear optical properties were carefully characterized and discussed. The most important study is that the formation mechanism of Ag quantum dots glass has also been discussed. And the results showed that the obtained materials are promising for applications in ultrafast all-optical switches and other optical devices.

2. Experiment

2.1. Stiff gels preparation

Fig. S1 is the photographs of Ag QDs NBS gel samples and Ag QDs NBS glasses obtained. The sodium borosilicate glass containing Ag nanocrystals (1.5 wt.%) was prepared by employing sol–gel method. All materials were analytical grade without further purification. The composition of the glass matrix was 5.74 Na_2O–21.38B_2O_3–72.88SiO_2 (in wt.%). Sodium borosilicate system glass containing silver nanocrystals was prepared by using tetraethyl orthosilicate (TEOS), boric acid (H_3BO_3), sodium ethylate (C_2H_5ONa) as precursors, methanol, 2-methoxyethanol, ethanol as precursor solvents, and hydrochloric acid as catalyst. The whole preparation procedure was

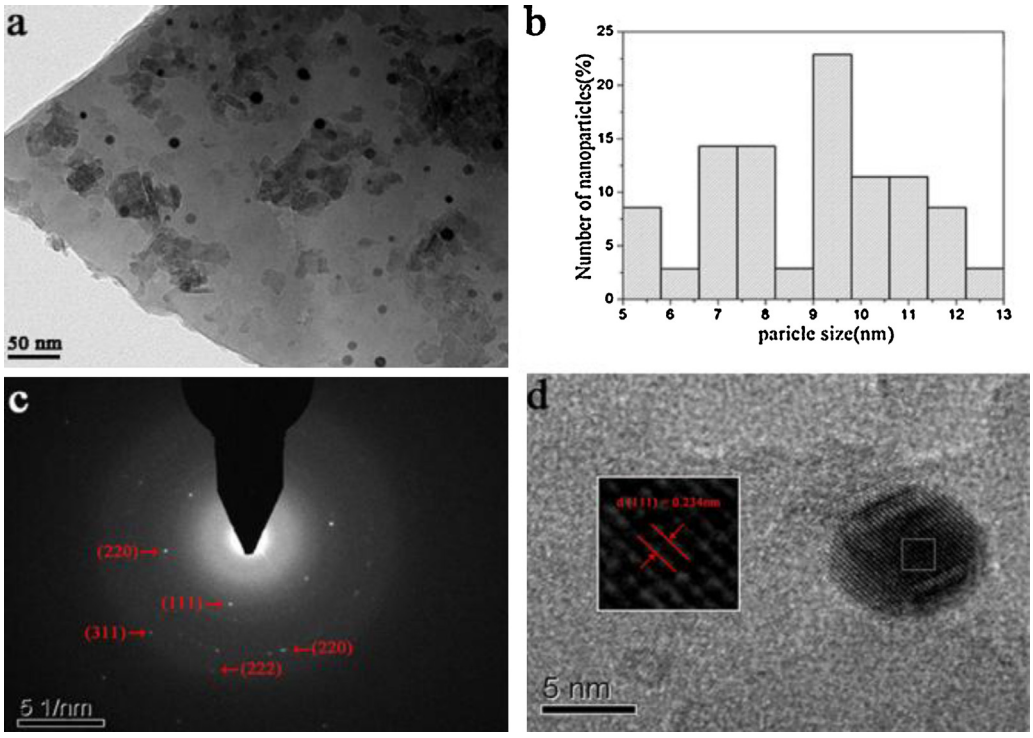

Fig. 2. TEM analysis of the Ag doped NBS glass (a) morphological image of TEM; (b) the size distribution image; (c) SAED image; (d) HRTEM image.

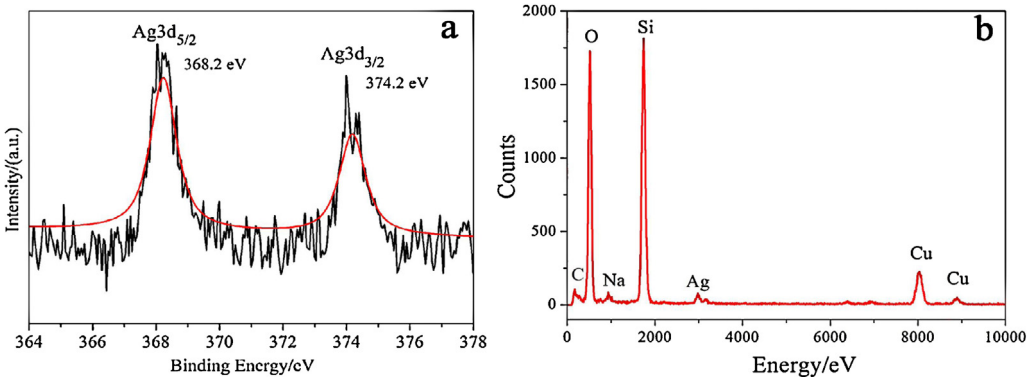

Fig. 3. (a) Characteristic XPS Spectrum of the Ag doped NBS glass. (b) EDX spectrum of the Ag doped NBS glass.

as follows: First, TEOS was added to ethanol solution, and deionized water and hydrochloric acid (pH 2) was added to the mixture. Then, the mixture was stirred vigorously for 1 h at room temperature. Next, H_3BO_3 solution and C_2H_5ONa solution were added to the mixture, after stirring for 1 h, a methanol solution containing of silver nitrate ($AgNO_3$, 99.99%) was added to above mixed solution. After 1 h stirring again, the homogeneous mixture solution was poured into a plastic container with volume of 10 mL which was then hermetically sealed and gelation proceeded for 5 days at room temperature to strengthen the gel network. The resultant gel was aged at 120 °C resulted in stiff gels after 2–3 weeks.

2.2. Ag QDs NBS glasses preparation

The stiff gel was heated in different atmosphere by the following steps:

a The stiff gel was heated in a tube furnace in oxygen (O_2) atmosphere with a heating rate of 10 °C/h up to 420/450/470 °C to decompose silver nitrate and eliminate organic residues. The loose and porous aerogel will form after the organic residues eliminated.
b The aerogel was held at 420/450/470 °C for 10 h by dry hydrogen (H_2) to form metallic Ag.
c The aerogel was sintered in nitrogen (N_2) atmosphere with a heating rate of 10 °C/h up to 600 °C, held at that temperature for 10 h to fully density, and cooled by turning off the heater power. The sodium borosilicate glasses containing Ag nanocrystals were obtained. The as-obtained glasses were cut and polished to a thickness of 1 mm for various measurements.

2.3. Characterization of the Ag QDs NBS glasses

The X-ray diffraction (XRD) patterns of the glasses were recorded with an X-ray diffractometer (Bruker D8 Advance) in the 2θ range 10–90° using Cu Kα radiation of wavelength l = 1.5406 Å. It was operated at 40 kV and 40 mA.

TEM, high-resolution TEM (HRTEM), and corresponding selected area electron diffraction (SAED) patterns of the as-prepared glasses were taken on a TEM (FEI Tecnai F20) performing with an acceleration voltage of 200 kV.

X-ray photoelectron spectroscopy (XPS) data were carried out using AXIS ULTRA DLD spectrometer, using monochrome Al Kα as the excitation source. Energy dispersive X-ray (EDX) spectra were collected using an Oxford INCA instrument attached to the field emission scanning electron microscope in the scanning range of 0–20 kV to analysis the chemical composition.

The optical absorption spectra of the glasses were measured in the wavelength range of 250–800 nm using a UV/vis spectrometer (UV-2450) at room temperature.

Nitrogen sorption isotherms and BJH pore size distribution curves of Ag doped NBS glass samples were recorded using a ASAP 2020 specific surface area and porosity analyzer after an outgassing process of several hours at 300 °C under secondary vacuum.

The third-order nonlinear susceptibility of the samples were measured by a single beam Z-scan technique [31]. NLO measurements with nonlinear absorption and nonlinear refraction of the glasses were investigated using a 76 MHz repetition rate mode-locked Ti:sapphire laser (Coherent Mira 900-D) with 200 fs pulse width at the wavelength of 800 nm.

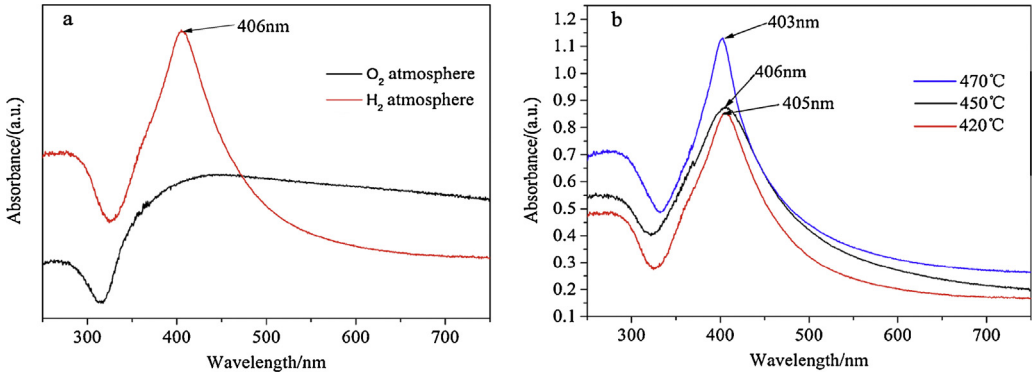

Fig. 4. The absorption spectra of the Ag doped NBS glass. (a) Effects of different atmosphere on absorption spectra of samples. (b) Effects of different heat temperature on absorption spectra of samples.

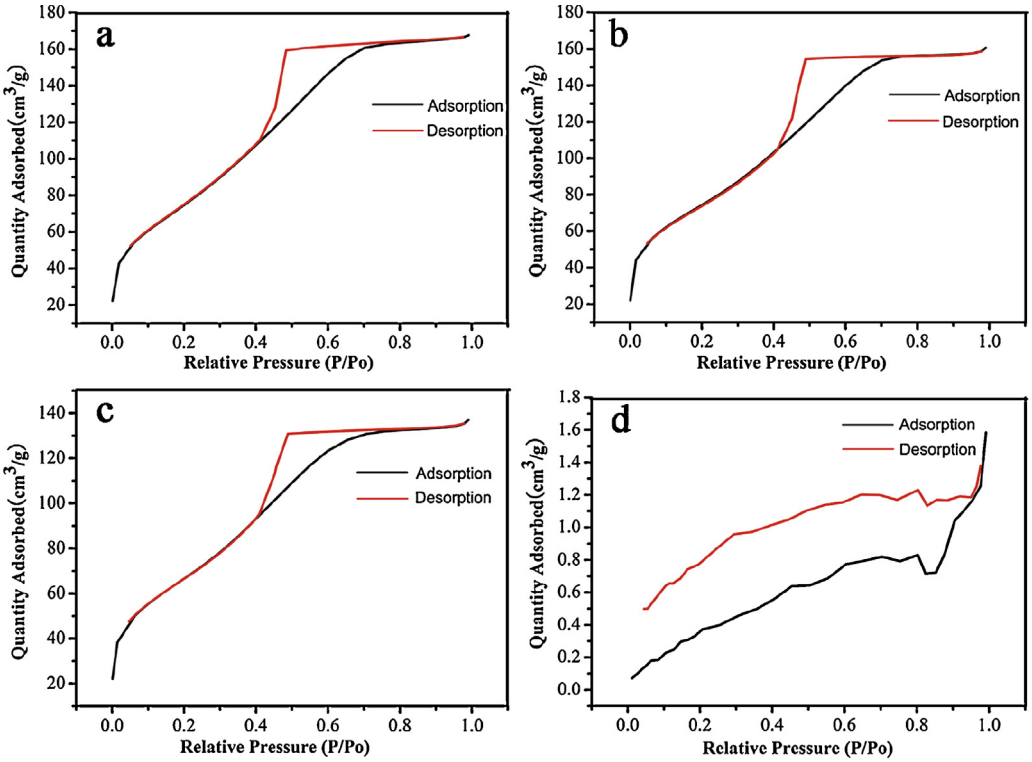

Fig. 5. Nitrogen adsorption–desorption isotherms of Ag doped NBS glasses stabilized at (a) 420 °C, (b) 450 °C, (c) 470 °C, (d) 600 °C.

3. Results and discussion

3.1. XRD analysis

Fig. 1(a–c) shows the XRD patterns of Ag doped sodium borosilicate glasses with Ag content of 1.5 wt.% and heat treatment with dry hydrogen (H_2) at 420 °C, 450 °C and 470 °C, respectively. The Joint Committee on Powder Diffraction Standards (JCPDS) pattern of silver is shown for comparison. Several clear peaks are observed in the pattern at $2\theta = 38.114$, 44.223, 64.420, 77.461, and 81.580 which are assigned to be reflections from the (111), (200), (220), (311) and (222) crystal planes,

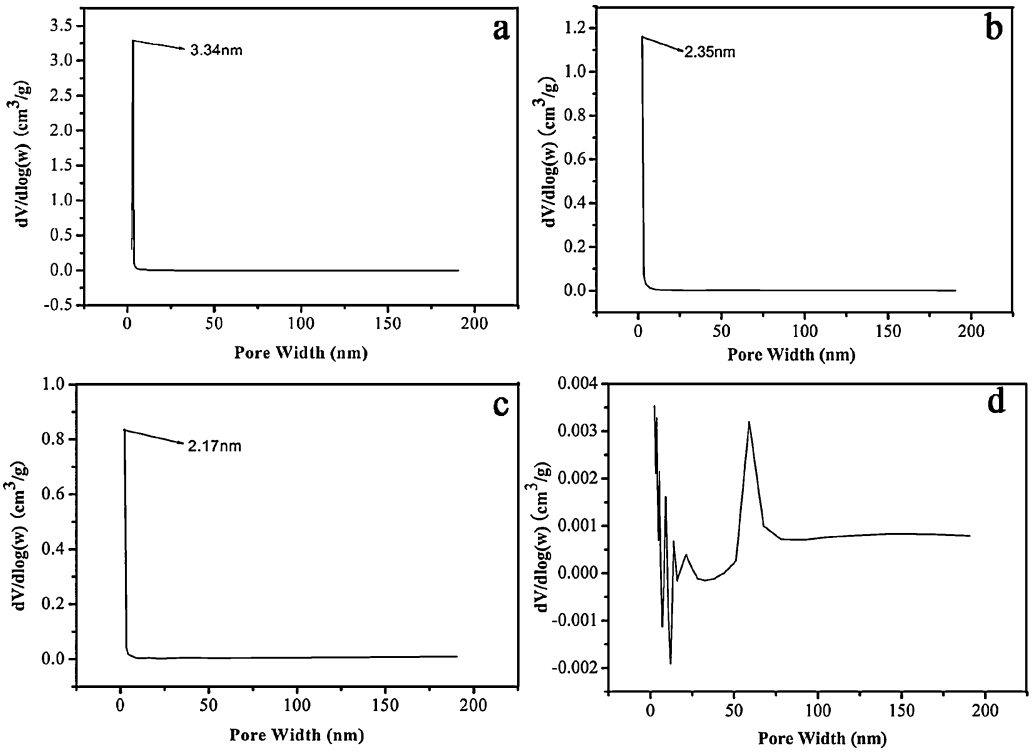

Fig. 6. BJH pore size distribution curves of Ag doped NBS glasses stabilized at (a) 420 °C, (b) 450 °C, (c) 470 °C, (d) 600 °C.

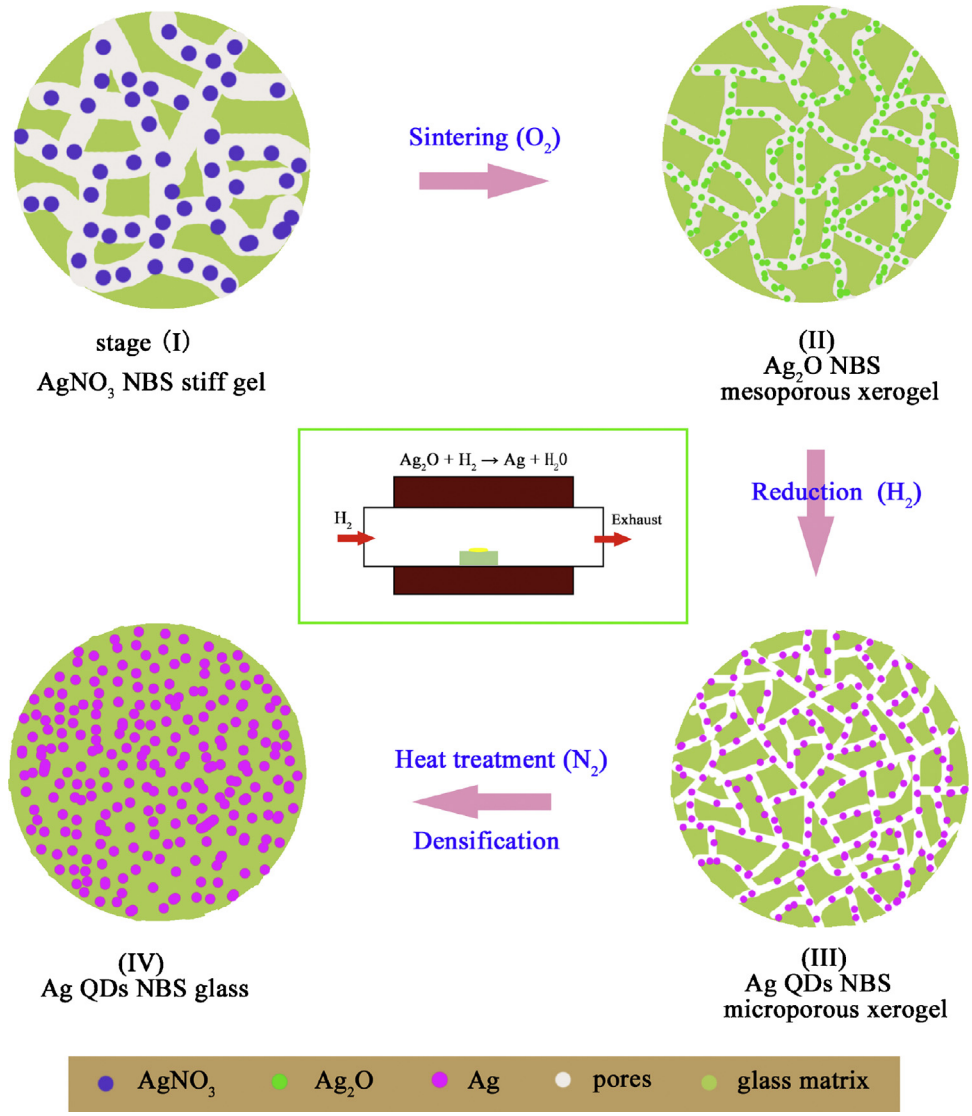

Scheme 1. A schematic illustration of the formation of the Ag QDs NBS glasses. The inset shows the apparatus for sintering Ag QDs NBS glasses.

respectively. All the diffraction peaks can be indexed as the cubic phase silver with lattice constants $a = 0.40857$ Å, which agree well with the value in the standard card (JCPDS card No. 65-2871). Furthermore, no peak for any impurity such as Ag_2O, or other phases is observed in the patterns which further confirm the crystalline and pure phase of the cubic silver. Moreover, the broad hump at a 2θ angle of 23° is assigned to the amorphous silica. With increasing the heat treatment temperature from 420 °C to 470 °C, the full width at half maximum gradually broadened, indicating that microcrystalline dimension of Ag nanocrystals can be controlled by the heated treatment due to Scherrer formula.

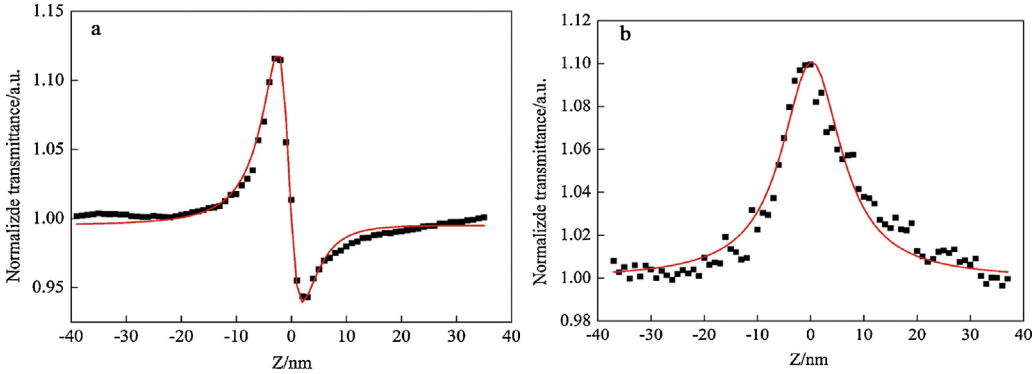

Fig. 7. (a) Z-scan curve of close aperture; (b) Z-scan curve of open aperture (circle dot is experimental data and solid line is theoretical curve).

3.2. TEM analysis

Fig. 2 shows the distribution and crystallinity of resulting Ag nanocrystals doped NBS glass with Ag content of 1.5 wt.% and heat treatment by dry hydrogen (H_2) at 450 °C. As shown in Fig. 2a, the TEM image clearly indicates that the high number density of silver nanocrystals with well controlled particle size distribution and uniformly dispersion have been embedded in amorphous glass matrix. The nanocrystals size distributions in Fig. 2b are extracted from the TEM image by using nano measurer. The average diameter of silver nanocrystals is about 8.5 ± 1 nm. From the SAED image in Fig. 2c, we can see that the diffraction patterns along with the amorphous diffuse ring pattern show several diffraction spots, which correspond to (1 1 1), (2 0 0), (2 2 0), (3 1 1) and (2 2 2) planes of the silver cubic phase. Fig. 2(d) shows the HRTEM image of the glass, depicting the atomic planes and confirming crystalline phase structure. The inset (in white square frames) is a partially enlarged detail showing the lattice fringe in Fig. 2(d). The distance of the lattice fringe spacing is 0.234 nm, which is in good agreement with the *d* spacing value of the plane (1 1 1) of silver in cubic crystal system (JCPDS No. 65-5871).

3.3. XPS and EDX analysis

Fig. 3a shows the surveyed X-ray photoelectron spectroscopy (XPS) spectra of the obtained glass. The narrow XPS spectrum of the silver nanocrystals in the glass matrix exhibits the characteristic double peaks with binding energies of 368.2 and 374.2 eV corresponding to Ag 3d5/2 and Ag 3d3/2, respectively, which are close to the standard values of metallic Ag [32]. This is a typical spectrum for the presence of the Ag^0 state. The chemical composition of Ag doped NBS glass was examined by energy dispersive X-ray spectrum (EDX) data (Fig. 3b). Ag signal in the spectra corresponds to Ag nanocrystals. Si, O, and Na signals correspond to the composition of the glass matrix, the strength of Ag signal is weak due to the influence of the strong signals of Si, O, and Na elements in EDX spectrum, while C and Cu element signals observed are due to the carbon coated copper grid. The presence of silver doped in the glass matrix was also confirmed by the silver peak in the EDS spectrum. All of these analysis results indicate that using both sol–gel and atmosphere control methods are highly effective for preparation of the sodium borosilicate glass containing Ag nanocrystals.

3.4. Optical absorption analysis

The most characteristic part of colloidal or nano silver is the surface plasmon resonance absorbance observable in the visible light regions [33,34]. The SPR effect occurs and produces a strong absorption peak if the frequency of the excitation wave is very close to the natural frequency of free conduction electrons of metal particles. The characteristics of the absorption are closely related to the shape, size, chemical composition and spatial organizations (e.g. solid or hollow) of the Ag nanocrystals [35]. Fig. 4(a) shows the absorption spectrum of glass sample sintered in different atmosphere, Fig. 4(a) shows the spectrum of Ag doped NBS glass heated in O_2 atmosphere. The Ag mainly exists in the form of ions, molecular clusters and Ag oxide. So no sharp SPR absorption peak appears in the surveyed wavelength range. Fig. 4(a–b) shows the absorption spectrum of glass sample heated at 450 °C in H_2 atmosphere. The SPR absorption peak of silver nanocrystals around 406 nm is observed, which is consistent with the predictions of Mie theory by Aden and Kerker [36]. Meanwhile, the surface plasma band at 406 nm is a clear evidence for Ag nanocrystals presence. We further investigated the effects of heat treatment temperature on SPR peak in H_2 atmosphere, the heat treatment were performed at 420, 450 and 470 °C, respectively. The results are showed in Fig. 4(b). With the increase of processing temperature, the intensity of peaks likely increases, and the full width at half-maximum (fwhm) of the SPR peaks decreases, in addition, the SPR peak position exhibits small shifts. It is probably due to the adjacent silver nanoparticles aggregates with the increases of processing temperature, lead to the volume fraction of Ag nanoparticles increase [37]. Owing to the heat treatment temperature difference is small, the influence is not noticeable.

4. Formation mechanism of Ag quantum dots in NBS glass matrix

To indirectly investigate the formation mechanism of Ag nanoparticles embedded in NBS glass matrix, pore distribution of obtained sample as the change of temperature was characterized using the nitrogen adsorption–desorption technique. Fig. 5 presents the nitrogen adsorption–desorption isotherms and Fig. 6 presents BJH pore size distribution curves of obtained samples at four different temperatures. The nitrogen adsorption–desorption isotherm profile of the obtained sample heated at 420 °C, 450 °C, 470 °C corresponds to typical type-IV curves, which reveals a mesoporous structure. The hysteresis loops have an H2 character, which matches with filling and emptying of mesopores through capillary condensation in mesoporous solids with pore interconnectivity, according to the IUPAC classification [38]. The pore size distribution obtained by the BJH method of sample at 420 °C, 450 °C, 470 °C, are centered on 3.34, 2.35, 2.17 nm, respectively, the BET surface area and pore total volume of the Ag nanoparticle obtained samples are about 286.66, 273.45, 246.4 $m^2 g^{-1}$ and 0.2592, 0.2406, 0.2118 $cm^3 g^{-1}$, respectively, indicating the presence of mesopores in the obtained samples. On the other hand, it is clearly seen that the pore shrinking with increasing the sintering temperature. It is worth noting that the nitrogen adsorption–desorption isotherm profile of obtained sample at 600 °C is irregular, at the same time, the ordinate values of BJH pore size distribution curves is negligible, meaning that the sample is non-porous. The reason is that the glass transition temperature Tg of NBS glass matrix is about 565 °C [38], so the sample has densification at 600 °C.

Based on above experimental results, a possible formation mechanism of Ag quantum dots NBS glass is proposed as follows. The formation of Ag quantum dots is observed step by step in this work, and a schematic representation of formation process is depicted in Scheme 1.

The hydrolysis, polycondensation and aging of NBS precursors occurred successfully, leading to the formation of the Ag precursor ($AgNO_3$) which was dispersed in the NBS stiff gel system (see stage I in the model). After heated in a tube furnace in oxygen (O_2) atmosphere, the loose and porous NBS xerogel could form due to organic substances being removed, meanwhile, the silver nitrate could be decomposed to Ag_2O.

$$AgNO_3 \rightarrow Ag_2O + NO_2 \uparrow \quad (1)$$

In the stage II, the aerogel undergoes heat treatment by dry hydrogen (H_2). With increasing the treatment temperature, Ag_2O dispersed in mesoporous NBS easily react with H_2 gas, the reaction

$$Ag_2O + H_2 \rightarrow Ag + H_2O \uparrow \quad (2)$$

would occur and the size of the as-formed Ag nanosphere is very small. Further prolonging the reaction time can result in the growth of the primary Ag nanosphere. Therefore, Ag quantum dots with different size can be controlled by varying the reaction time. When the content of [Ag] was kept at a constant value, increasing reduction temperature in reducing atmospheres, due to the pore shrinking, the size of as-form primary Ag nanocrystals decreases

and the aggregation of Ag nanosphere could be suppressed, which is consistent with XRD observations. Therefore, the total size of the Ag nanosphere can also be controlled by varying the reduction temperature. In this process, the interconnected pores are continuing to contract and this leads to the formation of a microporous space network frame structure of NBS xerogel matrix.

In the stage III, the aerogel was sintered in nitrogen (N_2) atmosphere to 600 °C to reach full densification. Finally, the creak-free monoliths NBS glasses containing Ag nanocrystals are obtained with a good transparency and mechanical strength (see stage IV in the model).

5. Third-order nonlinear optical absorption analysis

The nonlinear optical measurements of Ag doped NBS glass heated treatment in H_2 atmosphere at 450 °C is performed using a single beam Z-scan technique with the wavelength of 800 nm and laser pulses are 200 fs wide. Fig. 7 shows the Z-scan curves of (a) the closed-aperture ($S < 1$) and (b) the open-aperture ($S = 1$) of the glass, respectively. In Fig. 7(a), it is clearly seen that the close-aperture Z-scan curve with prefocal peak and postfocal valley, meaning that a self-defocusing process and a negative sign of nonlinear refraction. Meanwhile, the closed-aperture is asymmetric which indicates that both the nonlinear absorption and the nonlinear refraction take place simultaneously. Fig. 7(b) shows that the open-aperture is symmetric with respect to the focus ($z = 0$). open Z-scan can measure intensity-dependent nonlinear absorption. At the focus the irradiance is the greatest and thus will lead to the greater effect. If open Z-scan will produce a symmetrical transmittance peak-shaped curve, meaning that photo-induced transparency due to saturable absorption [28]. Hence, the nonlinear absorption belongs to saturable absorption (SA) performance in the glass.

Furthermore, we can observe from Tables S1 that the third-order nonlinear susceptibility of indium nanocrystals doped in sodium borosilicate is about 1.01×10^{-11} esu, which is four or five orders of magnitude larger than pure sodium borosilicate glass ($\chi^{(3)} \approx 10^{-15}$ esu). It shows that the $\chi^{(3)}$ of the composite materials can be strongly enhanced by the embedding Ag nanoparticles in the glass matrix. Furthermore, the third order nonlinear absorption effect of glass is obvious, the main causes of this phenomenon attributed to Ag quantum dots electronic effect. When the excitation frequency is close to SPR frequency, as for the case of Ag nanocrystals in our experiment when excited at 406 nm, part of the energy is absorbed in the Ag nanocrystals. Part of the absorbed energy promotes intraband transition ($4d \rightarrow 5s$ for Ag) between filled and empty states in the conduction band, and interband transition between the spatially localized d bands and the free-electron like conduction band. Typically, intraband transition is closely related to size. Generally, for metal nanoparticles of smaller than 10 nm, the intraband transitions, as a result of an electric dipole transition due to the confinement of the free electrons. The obtained Ag nanocrystals in our experiment with an average size of 8.5 ± 1 nm. Hence, intraband transitions result in a certain influence on the nonlinear absorption [39,40].

To induce the interband transition, the photon energy should be larger than that of the gap, the smallest gap energies of Ag is 4.0 eV [39], In our experiments of Z-scan, the excitation wavelength is 800 nm, corresponding to the photon energy of 1.55 eV, which is far less than 4.0 eV. The excitation intensity is relatively weak, the saturation phenomenon of the interband transitions cannot occur even if the interband transitions are induced by the two-photon absorption, accordingly $\mathrm{Im}\chi^{(3)}$ can only be positive [40]. To sum up, the intraband transitions of Ag nanocrystals dominate the nonlinear absorption effect. In addition, hot-electron contribution and the thermal conductivity of sodium borosilicate glass matrix [41] also influence the third-order nonlinear optical properties.

6. Conclusions

In summary, we have demonstrated the preparation of uniform spherical shape Ag nanoparticles embedded in sodium borosilicate monolithic transparent glass with Ag content of 1.5 wt.% by using sol–gel method. The average size of Ag nanocrystals is measured to be 8.5 ± 1 nm. The Ag surface plasma resonance absorption peak appear around 406 nm, the intensity of SPR absorption peak is changed with different heat treatment temperatures. Z-scan measurements show that the third-order optical nonlinear susceptibility of the glass is determined 1.01×10^{-11} esu and the mechanism of the nonlinear absorption is strongly dependent on the interband transitions. Furthermore, a possible formation mechanism of Ag quantum dots NBS glass is proposed. We anticipate that the research would also provide new and highly valuable information for the applications of this material in optical devices, such as optical switches and limiters. The sol–gel and atmosphere control methods not only provides a promising road for synthesis of Ag nanocrystals, but also can be useful to prepare other functional composite material. Additionally, further studies are in progress to better understand and control the optical and electronic structure of this material.

Acknowledgments

The work was financially supported by the National Natural Science Foundation of China (51272059); National Youth Science Foundation of China(51202166); Zhejiang Province Key Scientific and Technological Innovations Team of China (2009R50010).

Appendix A. Supplementary data

Supplementary data associated with this article can be found, in the online version, at http://dx.doi.org/10.1016/j.materresbull.2014.06.034.

References

[1] D.A.B. Miller, Are optical transistors the logical next step? Nat. Photonics 4 (2010) 3–5.
[2] D. Cotter, R.J. Manning, K.J. Blow, A.D. Ellis, A.E. Kelly, D. Nesset, I.D. Philips, A.J. Poustie, D.C. Rogers, Nonlinear optics for high-speed digital information processing, Science 286 (1999) 1523–1528.
[3] D.M. Da Silva, L.R.P. Kassab, S.R. Lüthi, C.B. De Araújo, A.S.L. Gomes, M.J.V. Bell, Frequency upconversion in Er^{3+} doped PbO-GeO_2 glasses containing metallic nanoparticles, Appl. Phys. Lett. 90 (2007) 081913.
[4] G. Lin, F. Luo, H. Pan, M.M. Smedskjaer, Y. Teng, D. Chen, J. Qiu, Q. Zhao, Universal preparation of novel metal and semiconductor nanoparticle-glass composites with excellent nonlinear optical properties, J. Phys. Chem. C 115 (2011) 24598–24604.
[5] L.R.P. Kassab, F.A. Bomfim, J.R. Martinelli, N.U. Wetter, J.J. Neto, C.B. Araújo, Energy transfer and frequency upconversion in Yb^{3+}-Er^{3+}-doped PbO-GeO_2 glass containing silver nanoparticles, Appl. Phys. B 94 (2009) 239–242.
[6] T. Karakouz, B.M. Maoz, G. Lando, A. Vaskevich, I. Rubinstein, Stabilization of gold nanoparticle films on glass by thermal embedding, ACS Appl. Mater. Interf. 3 (2011) 978–987.
[7] J.G. Li, S.K. Cushing, J. Bright, F. Meng, T.R. Senty, P. Zheng, A.D. Bristow, N.Q. Wu, Ag@ Cu_2O core–shell nanoparticles as visible-light plasmonic photo-catalysts, ACS Catal. 3 (2013) 47–51.
[8] C.J. Murphy, T.K. Sau, A.M. Gole, C.J. Orendorff, J.X. Gao, L.F. Gou, S.E. Hunyadi, T. Li, Anisotropic metal nanoparticles: synthesis, assembly, and optical applications, J. Phys. Chem. B 109 (2005) 13857–13870.
[9] Y.C. Yang, Wei J.H. Wen J.W, R. Xiong, Pan C.X. Shi J, Polypyrrole-decorated Ag–TiO_2 nanofibers exhibiting enhanced photocatalytic activity under visible-light illumination, ACS Appl. Mater. Interf. 5 (2013) 6201–6207.
[10] L. Berti, A. Andrea, F. Paolo, DNA-templated photoinduced silver deposition, J. Am. Chem. Soc. 127 (2005) 11216–11217.
[11] M. Anindita, B. Sujit, K.D. Jugal, K.M. Samar, C. Krishnananda, D. Goutam, Ag–TiO_2 nanoparticle codoped SiO_2 films on ZrO_2 barrier-coated glass substrates with antibacterial activity in ambient condition, ACS Appl. Mater. Interf. 2 (2010) 2540–2546.
[12] H. Di, I. Atsushi, D.B. Daniel, T.W. David, Synthesis and characterization of antibacterial silver nanoparticle-impregnated rice husks and rice husk ash, Environ. Sci. Technol. 47 (2013) 5276–5284.

[13] C. Rui, Z.H. Bai, S. Peng, Y.J. Huang, D. Kim, H.D. Sun, Fluorescent pH sensor based on Ag@ SiO_2 core–shell nanoparticle, ACS Appl. Mater. Interf. 5 (2013) 5856–5860.
[14] W.L. Song, F. Veronica, A. Mehran, Formation of icosahedral gold nanocrystals on the glass surface, J. Phys. Chem. C 114 (2010) 12850–12854.
[15] J.L. Hu, L. Wang, W.P. Cai, Y. Li, H.B. Zeng, L.Q. Zhao, P.S. Liu, Smart and reversible surface plasmon resonance responses to various atmospheres for silver nanoparticles loaded in mesoporous SiO_2, J. Phys. Chem. C 113 (2009) 19039–19045.
[16] Y. Chang, Y. Lu, K. Chou, Enhancement of photoluminescence of different quantum dots by Ag@ SiO_2 core–shell nanoparticles, Mater. Res. Bull. 48 (2013) 2076–2078.
[17] P. Massé, S. Mornet, E. Duguet, M. Tréguer-Delapierre, S. Ravaine, A. Iazzolino, J. B. Salmon, J. Leng, Synthesis of size-monodisperse spherical Ag@ SiO_2 nanoparticles and 3-D assembly assisted by microfluidics, Langmuir 29 (2013) 1790–1795.
[18] L. Rainville, M. Dorais, D. Boudreau, Controlled synthesis of low polydispersity Ag@ SiO_2 core–shell nanoparticles for use in plasmonic applications, RSC Adv. 3 (2013) 13953–13960.
[19] Y.H. Deng, D. Qi, C.H. Deng, X.M. Zhang, D.Y. Zhao, Superparamagnetic high-magnetization microspheres with an Fe_3O_4@ SiO_2 core and perpendicularly aligned mesoporous SiO_2 shell for removal of microcystins, J. Am. Chem. Soc. 130 (2008) 28–29.
[20] H. Lu, H.F. Ju, Q. Yang, Z. Li, H.Y. Ren, X. Xin, G.Y. Xu, Synthesis of Ag@ SiO_2 hybrid nanoparticles templated by a Triton X-100)/1-hexanol/cyclohexane/H_2O water-in-oil microemulsion, CrystEngComm 15 (2013) 6511–6517.
[21] H. Choi, J. Lee, S. Ko, J. Jung, H. Park, S. Yoo, O. Park, J. Jeong, S. Park, Y. Kim, Multipositional silica-coated silver nanoparticles for high-performance polymer solar cells, J. Nano Lett. 13 (2013) 2204–2208.
[22] D. Faccio, P.D. Trapani, E. Borsella, F. Gonella, P. Mazzold, A.M. Malvezz, Measurement of the third-order nonlinear susceptibility of Ag nanoparticles in glass in a wide spectral range, Europhys. Lett. 43 (1998) 213.
[23] X.C. Yang, Z.W. Dong, H.X. Liu, J.X. Xu, S.X. Qian, Effects of thermal treatment on the third-order optical nonlinearity and ultrafast dynamics of Ag nanoparticles embedded in silicate glasses, Chem. Phys. Lett. 475 (2009) 256–259.
[24] D.B. Leonardo, E.C. Barbano, T.A. de Assumpção, L. Misoguti, L.R.P. Kassab, S.C. Zilio, Femtosecond third-order nonlinear spectra of lead–germanium oxide glasses containing silver nanoparticles, Opt. Express (20 2012) 6844–6850.
[25] K. Babooram, R. Narain, Fabrication of SWNT/silica composites by the sol–gel Process, ACS Appl. Mater. Interf. 1 (2009) 181–186.
[26] J.J. Allen, E. Rosenberg, E. Johnston, C. Hart, Sol–gel synthesis and characterization of silica polyamine composites: applications to metal ion capture, ACS Appl. Mater. Interf. 4 (2012) 1573–1584.
[27] R. Ciriminna, A. Fidalgo, V. Pandarus, F. Béland, L.M. Ilharco, M. Pagliaro, The sol–gel route to advanced silica-based materials and recent applications, Chem. Rev. 113 (2013) 6592–6620.
[28] J.S. Zhong, W.D. Xiang, H.J. Zhao, Z.P. Chen, X.J. Liang, W.G. Zhao, G.X. Chen, Preparation and nonlinear optical properties of indium nanocrystals in sodium borosilicate glass by the sol–gel route, Mater. Res. Bull. 47 (2012) 3691–3696.
[29] J.S. Zhong, W.D. Xiang, H.J. Zhao, W.G. Zhao, G.X. Chen, X.J. Liang, Synthesis, characterization, and nonlinear optical properties of copper quantum dots embedded in sodium borosilicate glass, J. Alloys Compd. 537 (2012) 269–274.
[30] X.Y. Yang, W.D. Xiang, T. Liu, H.J. Zhao, X.Y. Zhang, X.J. Liang, Microstructures and the third-order optical nonlinearities of semimetal Bi nanocrystals in the sodium borosilicate glass, Mater. Lett. 65 (2011) 1959–1962.
[31] M. Sheik-Bahae, A.A. Said, D.J. Hagan, Sensitive measurement of optical nonlinearities using a single beam, IEEE J. Quantum Elect. 26 (1990) 760–769.
[32] S. Hüfner, G.K. Wertheim, J.H. Wernick, XPS core line asymmetries in metals, Solid State Commun. 17 (1975) 417–422.
[33] K.H. Chen, Y.C. Pu, K.D. Chang, Y.F. Liang, C.M. Liu, J.W. Yeh, H.C. Shih, Y.J. Hsu, Ag-nanoparticle-decorated SiO_2 nanospheres exhibiting remarkable plasmon-mediated photocatalytic properties, J. Phys. Chem. C 116 (2012) 19039–19045.
[34] H.Y. Liang, Z.P. Li, W.Z. Wang, Y.S. Wu, H.X. Xu, Highly Surface-roughened "Flower-like" silver nanoparticles for extremely sensitive substrates of surface-enhanced Raman scattering, Adv. Mater. 21 (2009) 4614–4618.
[35] D.D. Evanoff, G. Chumanov, Size-controlled synthesis of nanoparticles. 2. Measurement of extinction, scattering, and absorption cross sections, J. Phys. Chem. B 108 (2004) 13957–13962.
[36] A.L. Aden, M. Kerker, Scattering of electromagnetic waves from two concentric spheres, J. Appl. Phys. 22 (1951) 1242.
[37] Y. Teng, J.J. Zhou, F.F. Luo, G. Lin, J.R. Qiu, Controllable space selective precipitation of copper nanoparticles in borosilicate glasses using ultrafast laser irradiation, J. Non-Cryst. Solids 357 (2011) 2380–2383.
[38] K.S.W. Sing, H. Everettd, R.A.W. Haul, L. Moscou, R.A. Pierotti, J. Rouquerol, T. Siemieniewska, Physical and biophysical chemistry division commission on colloid and surface chemistry including catalysis, Pure Appl. Chem. 57 (1985) 603–619.
[39] S.L. Qu, Y.W. Zhang, H.J. Li, J.R. Qiu, C.S. Zhu, Nanosecond nonlinear absorption in Au and Ag nanoparticles precipitated glasses induced by a femtosecond laser, Opt. Mater. 28 (2006) 259–265.
[40] C. Voisin, F.N. Del, D.C.F. Vallee, Ultrafast electron dynamics and optical nonlinearities in metal nanoparticles, J. Phys. Chem. B 105 (2001) 2264–2280.
[41] X.Y. Yang, W.D. Xiang, H.J. Zhao, T. Liu, X.Y. Zhang, X.J. Liang, Nonlinear saturable absorption of the sodium borosilicate glass containing Bi_2S_3 nanocrystals using Z-scan technique, J. Alloys Compd. 509 (2011) 7283–7289.